Mid-Pliocene hominin diversity revisited

Hester HANEGRAEF, Meave G. LEAKEY,
Louise N. LEAKEY & Fred SPOOR

LUCY'S HEIRS – TRIBUTE TO YVES COPPENS

Edited by Jean-Jacques HUBLIN, Aurélien MOUNIER & Nicolas TEYSSANDIER

PUBLICATIONS SCIENTIFIQUES

MUSÉUM NAL HIST NATURELLE

Couverture / *Cover*:
Made from the Figures of the article.

Comptes Rendus Palevol est indexé dans / Comptes Rendus Palevol *is indexed by:*
– Cambridge Scientific Abstracts
– Current Contents® Physical
– Chemical, and Earth Sciences®
– ISI Alerting Services®
– Geoabstracts, Geobase, Georef, Inspec, Pascal
– Science Citation Index®, Science Citation Index Expanded®
– Scopus®.

Les articles ainsi que les nouveautés nomenclaturales publiés dans *Comptes Rendus Palevol* sont référencés par /
Articles and nomenclatural novelties published in Comptes Rendus Palevol *are registered on:*
– ZooBank® (http://zoobank.org)

Mid-Pliocene hominin diversity revisited

Hester HANEGRAEF
Centre for Human Evolution Research, Natural History Museum,
Cromwell Road, SW7 5BD London (United Kingdom)
h.hanegraef@nhm.ac.uk (corresponding author)

Meave G. LEAKEY
Turkana Basin Institute, Department of Anthropology, Stony Brook University,
Circle Road, Stony Brook, NY 11794-4364 (United States)
meaveleakey@gmail.com

Louise N. LEAKEY
Turkana Basin Institute, Department of Anthropology, Stony Brook University,
Circle Road, Stony Brook, NY 11794-4364 (United States)
and Department of Earth Sciences, National Museums of Kenya, Museum Hill, Nairobi (Kenya)
louiseleakey@gmail.com

Fred SPOOR
Centre for Human Evolution Research, Natural History Museum,
Cromwell Road, SW7 5BD London (United Kingdom)
and Department of Human Origins, Max Planck Institute for Evolutionary Anthropology,
Deutscher Platz 6, 04103 Leipzig (Germany)
f.spoor@nhm.ac.uk (corresponding author)

ABSTRACT

Geometric morphometric analyses are used to examine the maxillary shape of the *Kenyanthropus platyops* Leakey, Spoor, Brown, Gathogo, Kiarie, Leakey & McDougall, 2001 holotype KNM-WT 40000 and the *Australopithecus deyiremeda* Haile-Selassie, Gilbert, Melillo, Ryan, Alene, Deino, Levin, Scott & Saylor, 2015 holotype BRT-VP-3/1, expanding on the work of Spoor *et al.* (2010, 2016) by using more accurate data and a larger comparative sample. The main objective is to assess whether these two specimens differ from the contemporary taxon *Australopithecus afarensis* Johanson, White & Coppens, 1978 and more broadly from species of *Australopithecus* Dart, 1925 and *Paranthropus* Broom, 1938, as well as from each other. Five two-dimensional landmarks recorded on virtual models obtained from

computed tomography scans quantify key features of the maxilla used in the differential diagnoses of *K. platyops* and *A. deyiremeda*. Principal component analyses were performed to describe shape differences, and the magnitudes of these differences and their statistical significance were assessed using Procrustes and Mahalanobis distances, respectively. The maxillary shapes of both KNM-WT 40000 and BRT-VP-3/1 are significantly different from *A. afarensis*, the former more so than the latter, and they differ from *A. afarensis* in dissimilar ways. Where KNM-WT 40000 has a more anterosuperiorly positioned zygomatic process with a longer, more orthognathic, and transversely flat subnasal clivus than *A. afarensis*, the shape difference of BRT-VP-3/1 is best described as a posterior shift (retraction) of the entire dental arcade. The findings of this study quantitatively support the species status of *K. platyops* and *A. deyiremeda*, and corroborate the notion that hominin diversity extended well into the mid-Pliocene of eastern Africa.

RÉSUMÉ
Retour sur la diversité des hominines du Pliocène moyen.
À l'aide d'analyses de morphométrie géométrique, nous examinons la conformation des maxillaires de KNM-WT 40000, l'holotype de *Kenyanthropus platyops* Leakey, Spoor, Brown, Gathogo, Kiarie, Leakey & McDougall, 2001, et BRT-VP-3/1, l'holotype d'*Australopithecus deyiremeda* Haile-Selassie, Gilbert, Melillo, Ryan, Alene, Deino, Levin, Scott & Saylor, 2015. Cette étude approfondit les travaux antérieurs de Spoor *et al.* (2010, 2016) en utilisant des données plus précises et un échantillon comparatif plus important. L'objectif principal est d'évaluer si ces deux spécimens diffèrent non seulement l'un de l'autre, mais également du taxon contemporain *Australopithecus afarensis* Johanson, White & Coppens, 1978, ainsi que des espèces d'*Australopithecus* Dart, 1925 et de *Paranthropus* Broom, 1938 en général. Cinq landmarks placés sur des projections bidimensionnelles de modèles virtuels obtenus par tomodensitométrie quantifient les caractéristiques clés du maxillaire utilisées dans les diagnoses différentielles de *K. platyops* et *A. deyiremeda*. Des analyses en composantes principales nous permettent de décrire les différences de conformation et l'ampleur de ces différences ainsi que leur significativité statistique, qui sont respectivement évaluées à l'aide de distances Procrustes et de Mahalanobis. Les conformations des maxillaires de BRT-VP-3/1, et surtout de KNM-WT 40000, diffèrent significativement de celles d'*A. afarensis*, et ce, de façons distinctes. Alors que KNM-WT 40000 a un processus zygomatique positionné plus antéro-supérieurement avec un clivus subnasal plus long, plus orthognathe et transversalement plus plat qu'*A. afarensis*, la différence de conformation observée entre BRT-VP-3/1 et *A. afarensis* se caractérise principalement par un déplacement postérieur (rétraction) de l'ensemble de l'arcade dentaire. Les résultats quantitatifs de cette étude supportent la validité des espèces *K. platyops* et *A. deyiremeda*, corroborant ainsi l'idée qu'une importante diversité au sein des hominines était déjà en place au Pliocène moyen en Afrique de l'Est.

INTRODUCTION

Our understanding of human evolution in the mid-Pliocene (*c.* 3-4 Myr) has dramatically changed over the last two decades. During the 1980s and 1990s a consensus view emerged that the species *Australopithecus afarensis* Johanson, White & Coppens, 1978 and its likely ancestor, *Australopithecus anamensis* Leakey, Feibel, McDougall & Walker, 1995, formed the single hominin lineage present during that time interval (see Kimbel & Delezene 2009 for a review). *Australopithecus bahrelghazali* Brunet, Beauvilain, Coppens, Heintz, Moutaye & Pilbeam, 1996 was named based on 3.6 Myr fossils from Chad (Lebatard *et al.* 2008), but this interpretation has received little acceptance because the diagnostic distinction from *A. afarensis* is commonly perceived as insufficient (Kimbel 2015; Wood & Grabowski 2015). However, with the announcement of the new 3.3 to 3.5 Myr species *Kenyanthropus platyops* Leakey,

Spoor, Brown, Gathogo, Kiarie, Leakey & McDougall, 2001 and *Australopithecus deyiremeda* Haile-Selassie, Gilbert, Melillo, Ryan, Alene, Deino, Levin, Scott & Saylor, 2015 as well as the as-yet unassigned 3.4 Myr partial hominin foot from Burtele (Haile-Selassie *et al.* 2012) further evidence emerged that the mid-Pliocene of eastern Africa showed more taxic diversity than originally assumed (Fig. 1; Spoor 2015; Wood & Boyle 2016; Haile-Selassie *et al.* 2016).

The poor preservation of the *K. platyops* holotype cranium KNM-WT 40000 triggered the anecdotal criticism that the perceived differences from *A. afarensis* were caused by deformation (White 2003). However, a detailed analysis of the facial distortion and its impact on the morphology, followed by comparative analyses of the deformation-corrected maxilla confirmed the distinctiveness of *K. platyops* from other early hominin species (Spoor *et al.* 2010). Following the naming of *A. deyiremeda*, its holotype maxilla BRT-VP-3/1 was
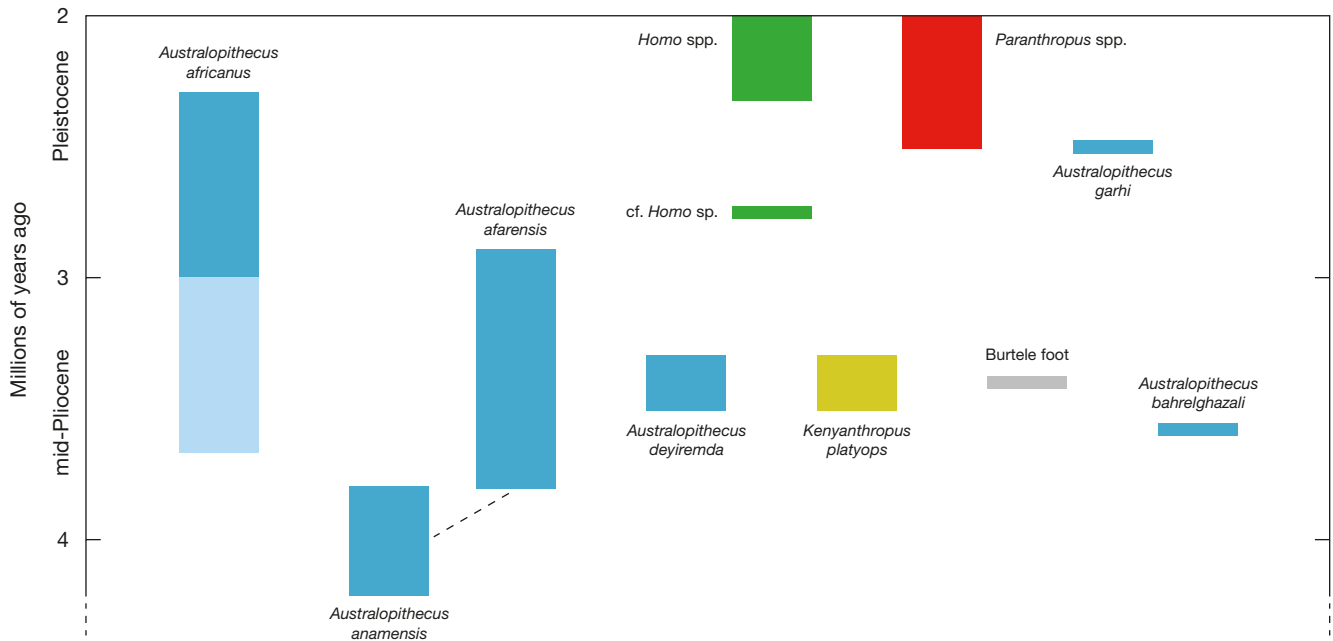
FIG. 1. — Temporal distribution of known Plio-Pleistocene hominin species, including those attributed to *Australopithecus* Dart, 1925 (**blue**), *Kenyanthropus* Leakey, Spoor, Brown, Gathogo, Kiarie, Leakey & McDougall, 2001 (**yellow**), *Homo* Linnaeus, 1758 (**green**), and *Paranthropus* Broom, 1938 (**red**). The **light blue area** represents a possible earlier age range for *A. africanus* Dart, 1925 (Granger *et al.* 2022). The evolutionary divergence of *A. afarensis* Johanson, White & Coppens, 1978 from *A. anamensis* Leakey, Feibel, McDougall & Walker, 1995 remains uncertain, as indicated by the **dashed black line**.

added to the two-dimensional (2D) geometric morphometric analyses of the latter study, leading to the conclusion that it differs substantially from the maxillae of both *K. platyops* and *A. afarensis* (Spoor *et al.* 2016). Although the results of these analyses have not been queried in the literature, they had some weaknesses that we now aim to remedy in the current study.

The 2D landmarks characterising the maxillary morphology in Spoor *et al.* (2010, 2016) were mostly taken from digital camera images showing the specimens in lateral view, with markers indicating the frequently obscured points nasospinale and prosthion (Fig. 2B). Apart from minor inaccuracies introduced by parallax artefacts, a major drawback was that the fossils in the comparative sample could only be photographed in their preserved state, so that any distortion could only be corrected by intuitive adjustment of landmark positions in the images. In addition, not all known *A. afarensis* maxillae could be included at the time, as the images of the fossils had been made in 2000.

Since the publication of Spoor *et al.* (2010, 2016), micro-computed tomography (CT) scans have been made of all available *A. afarensis* maxillae from Hadar. These were used in a detailed study, which assessed distortion and missing parts, correcting three-dimensional (3D) virtual models accordingly (see Fig. 2C for an example) as the basis for comparative geometric morphometric analyses of maxillary variation in both *A. afarensis* and extant hominine species (Hanegraef *et al.* 2022; Hanegraef 2023). After extending this micro-CT based approach to samples of other early hominin taxa, this work can now be used to revisit the original analyses in Spoor *et al.* (2010, 2016), comparing the maxillae of *K. platyops* and *A. deyiremeda*.

One limitation of these original analyses, that they were done in 2D rather than in full 3D, cannot be improved on here because the distortion of the KNM-WT 40000 maxilla could only be corrected in left lateral view. The objectives of the present study combine those outlined in Spoor *et al.* (2010, 2016), exploring whether the KNM-WT 40000 and BRT-VP-3/1 holotypes are different in maxillary shape from contemporary *A. afarensis* and other australopiths, as well as different from each other.

MATERIAL AND METHODS

The KNM-WT 40000 and BRT-VP-3/1 maxillae are compared with *A. anamensis* (KNM-KP 29283), *A. afarensis* (A.L. 199-1, A.L. 200-1a, A.L. 417-1d, A.L. 427-1a, A.L. 442-1, A.L. 444-2a, A.L. 486-1, A.L. 822-1, A.L. 922-1), *Australopithecus africanus* Dart, 1925 (MLD 9, Sts 5, Sts 52, Sts 71, StW 573), *Paranthropus aethiopicus* (Arambourg & Coppens, 1968) (KNM-WT 17000), *Paranthropus boisei* (Leakey, 1959) (OH 5), and *Paranthropus robustus* Broom, 1938 (DNH 7, SK 11, SK 12, SK 13, SK 46, SKW 11). All specimens are adults, except for A.L. 486-1, Sts 52, OH 5, SK 13, and SKW 11, which are late juveniles with their third molars not in occlusion. BRT-VP-3/1 is classified as a young adult (Haile-Selassie *et al.* 2015) and probably falls in the latter category as well. Specimens previously analysed in Spoor *et al.* (2010, 2016) but not included here, were deemed too distorted (StW 498, SK 48, and SK 83), or lacked 3D scan data (BOU-VP-12/130). Specimens newly included here are A.L. 442-1, A.L. 922-1, Sts 5, StW 573, and DNH 7.

Scanning procedures for KNM-WT 40000 and BRT-VP-3/1 are described in Spoor *et al.* (2010) and Haile-Selassie *et al.* (2015), respectively. The nine *A. afarensis* specimens were scanned with the portable Skyscan 1173 micro-CT scanner of the Department of Human Evolution at the Max Planck Institute for Evolutionary Anthropology in Leipzig, at the time installed at the National Museum of Ethiopia in Addis Ababa (isotropic voxel size: 0.03-0.07 mm). Other CT data of hominin fossils were obtained from the digital archives of the National Museums of Kenya in Nairobi, Witwatersrand University in Johannesburg, the Ditsong Museum in Pretoria, and the Department of Anthropology at the University of Vienna.

The measurement protocol is adapted from Spoor *et al.* (2010, 2016) and Hanegraef *et al.* (2022), using five 2D landmarks to capture the maxillary morphology (Fig. 2D). The landmarks comprise nasospinale (ns), prosthion (pr), the average of the distal canine alveolar margin and mesial third premolar alveolar margin (cp3), the distal second molar alveolar margin (m2), and the anteroinferior take-off of the zygomatic process (azp). The latter landmark is defined as the point most anterior, inferior, and medial on the root of the zygomatic process (Spoor *et al.* 2010; Hanegraef *et al.* 2022). These landmarks quantify the orientation and length of the subnasal clivus in the midplane (pr-ns), the position of the anterior zygomatic process along the postcanine tooth row (azp relative to cp3-m2), and the degree of anterior projection and transverse flatness of the subnasal clivus (pr-cp3).

Landmarks were newly recorded on 3D digital surface visualisations extracted from the CT scans using Avizo 7.1 (FEI Visualization Sciences Group). For the nine *A. afarensis* specimens, the landmarks were taken from the maxillae as reconstructed in Hanegraef (2023). For the remaining fossil sample, landmarks were collected on the left and right maxilla and then symmetrised when both sides are sufficiently preserved (KNM-KP 29283, Sts 5, KNM-WT 17000, OH 5, SK 11, SK 12, SK 13, SK 46). In those cases where one side is missing or affected by taphonomic distortion, landmarks were collected either on the left (KNM-WT 40000, BRT-VP-3/1, Sts 52) or right (MLD 9, Sts 71, StW 573, DNH 7, SKW 11) maxilla. The 3D landmarks were then projected onto the midplane established for each specimen based on its morphology. For KNM-WT 40000, landmarks were corrected for distortion of the specimen as described in Spoor *et al.* (2010). For BRT-VP-3/1, landmarks were collected from parallel-projected 3D surface views based on a CT scan of the original fossil as detailed in Spoor *et al.* (2016). In this study we use the best estimate of pr (version "a" in Spoor *et al.* 2016) and azp located at mesial fourth premolar level (version "b" in Spoor *et al.* 2016), as this is most consistent with the approach in Hanegraef *et al.* (2022).

A generalised Procrustes analysis of the landmark coordinates and principal component analyses (PCA) of the resulting shape variables were performed in R 4.3.2 (R Core Team 2023). The ensuing principal component (PC) plots describe the shape differences among KNM-WT 40000 and BRT-VP-3/1 in the setting of the wider hominin sample

and in the context of the *A. afarensis* specimens. Differences in shape are visualised using wireframes as defined in Figure 2D. All described differences relate to relative rather than absolute locations of landmarks with respect to each other given that size, orientation, and position have been removed in the analyses. Procrustes coordinates are provided in Appendix 1.

The magnitude of differences between the KNM-WT 40000 and BRT-VP-3/1 maxillae and the mean shape of those species represented by multiple specimens (i.e., *A. afarensis*, *A. africanus*, and *P. robustus*) was determined through Procrustes distances. The significance of these shape differences was assessed, albeit approximately given the small sample sizes, using Mahalanobis distances calculated from all non-zero PCs based on a chi-square distribution and the appropriate degrees of freedom (software written by Paul O'Higgins; see Spoor *et al.* 2016).

ABBREVIATIONS

Locality abbreviations

A.L.   Hadar, Ethiopia;
BOU-VP   Bouri, Middle Awash, Ethiopia;
BRT-VP   Burtele, Woranso-Mille, Ethiopia;
DNH   Drimolen Main Quarry, South Africa;
KNM-KP   Kanapoi, Kenya;
KNM-WT   West Turkana, Kenya;
MLD   Makapansgat, South Africa;
OH   Olduvai Gorge, Tanzania;
SK/SKW   Swartkrans, South Africa;
Sts/StW   Sterkfontein, South Africa.

Landmark abbreviations

azp   anteroinferior take-off of the zygomatic process;
cp3   average of the distal canine alveolar margin and mesial third premolar alveolar margin;
m2   distal second molar alveolar margin;
ns   nasospinale;
pr   prosthion.

Other abbreviations

2D   two-dimensional;
3D   three-dimensional;
CT   computed tomography;
PC   principal component;
PCA   principal component analysis.

RESULTS

In the PCA of the full sample, the first six PCs account for 100% of the shape variance. PCs 1, 2, 4, and 5 reveal relevant differences among the fossils, and these are shown in Figure 3, with the extreme shapes of each axis visualised using wireframes. PCs 1 and 2 jointly represent 83% of the variance, as opposed to only 9% for PCs 4 and 5 combined. However, the latter nevertheless deserve attention here, as they express characteristic morphology of KNM-WT 40000.

PC 1 (63% of total shape variance) separates *Australopithecus* Dart, 1925 species, with positive scores representing a more inferoposteriorly positioned zygomatic process,
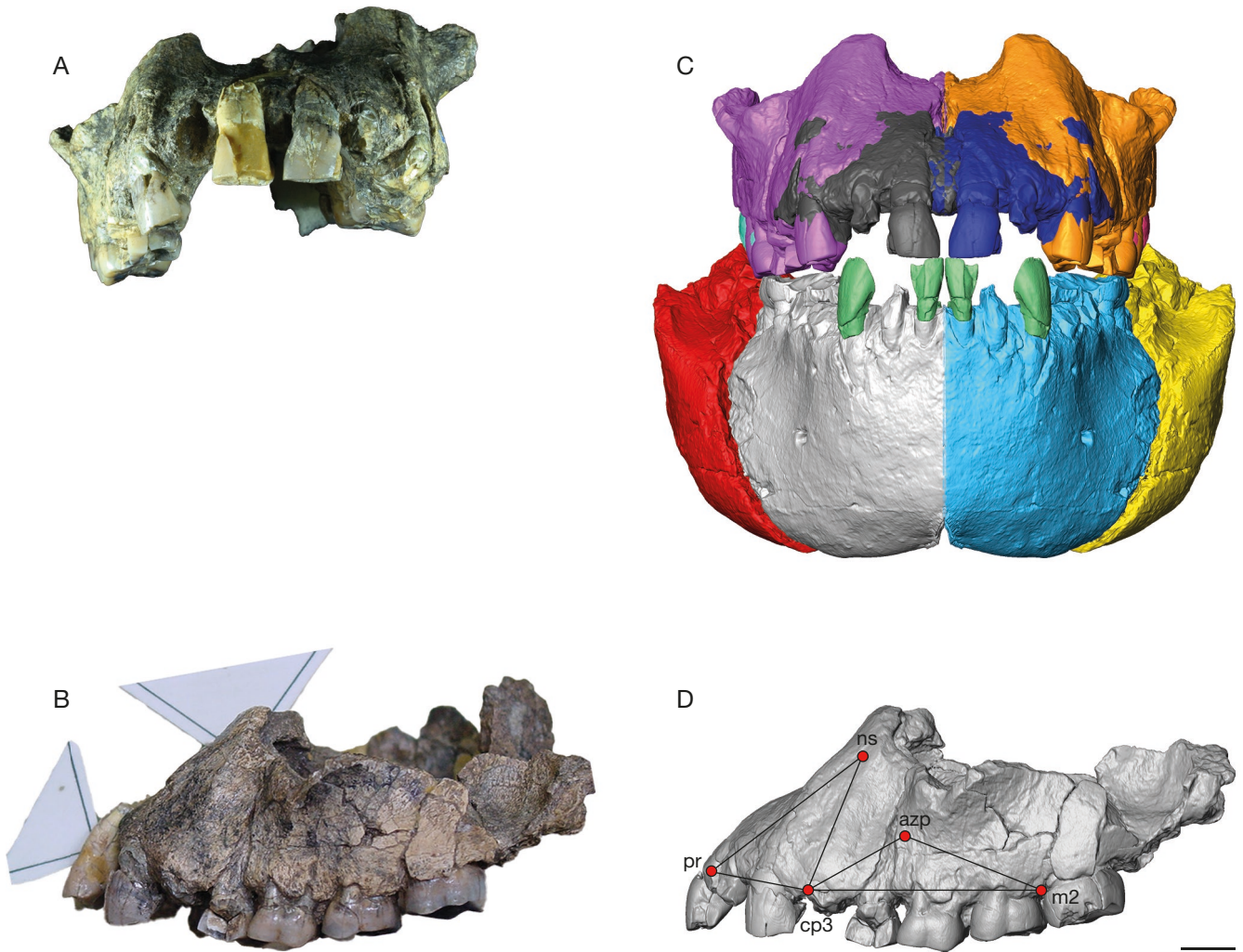
FIG. 2. — **A**, Frontal view of the A.L. 444-2a maxillae which display signs of significant postmortem distortion, including warping and crushing; **B**, lateral view of the A.L. 444-2a maxilla (**reversed right side**) as used in Spoor *et al.* (2010, 2016). The position of nasospinale and prosthion are not visible and are therefore indicated by markers; **C**, frontal view of the reconstructed A.L. 444-2 lower face with colours differentiating between fragments used in the reconstruction; **D**, lateral view of the reconstructed A.L. 444-2a maxilla showing the landmarks employed in this study together with the connecting wireframe used in Figures 3–5. Abbreviations: **azp**, anteroinferior take-off of the zygomatic process; **cp3**, average of the distal canine alveolar margin and mesial third premolar alveolar margin; **m2**, distal second molar alveolar margin; **ns**, nasospinale; **pr**, prosthion. Scale bar: 1 cm.

a more anteroinferiorly positioned nasal sill, and a shorter and transversely curved (projecting) subnasal clivus, from *Paranthropus* Broom, 1938 species, with negative scores representing a more anterosuperiorly positioned zygomatic process, a more posterosuperiorly positioned nasal sill, and a longer and transversely flat subnasal clivus (Fig. 3A). These shape differences describe the flattened anterior maxilla and relatively forwardly placed zygomatic root that distinguish *Paranthropus* from *Australopithecus* species. KNM-WT 40000 is intermediate between these two genera. BRT-VP-3/1 falls within the PC 1 range of the *Australopithecus* species considered in this study.

PC 2 (20% of total shape variance) separates specimens with a longer subnasal clivus and a more posterosuperiorly positioned nasal sill and zygomatic process on the negative end, from those with a shorter subnasal clivus and a more anteroinferiorly positioned nasal sill and zygomatic process on the positive end (Fig. 3A). *Australopithecus afarensis*, *A. africanus*,

and *Paranthropus* show a large range of PC 2-related morphological variation, while KNM-WT 40000 and *A. anamensis* have intermediate scores. On the other hand, BRT-VP-3/1 falls on the positive end, outside the range of any other specimen considered in this study.

PC 3 (6% of total shape variance) represents marked variation in relative inferosuperior position of the anterior zygomatic process, as well as some joint variation in the orientation of the subnasal and anterior alveolar segments relative to the postcanine part. All species largely overlap and both KNM-WT 40000 and BRT-VP-3/1 fall in the middle of the range.

PC 4 (5% of total shape variance) mostly represents marked variation in inferosuperior position of the nasal sill (nasospinale), with species of *Australopithecus* and *Paranthropus* overlapping substantially (Fig. 3B). KNM-WT 40000 has the second to highest score, expressing a relatively superior position of the nasal sill. BRT-VP-3/1 also shows one of the higher scores, but less so than KNM-WT 40000.
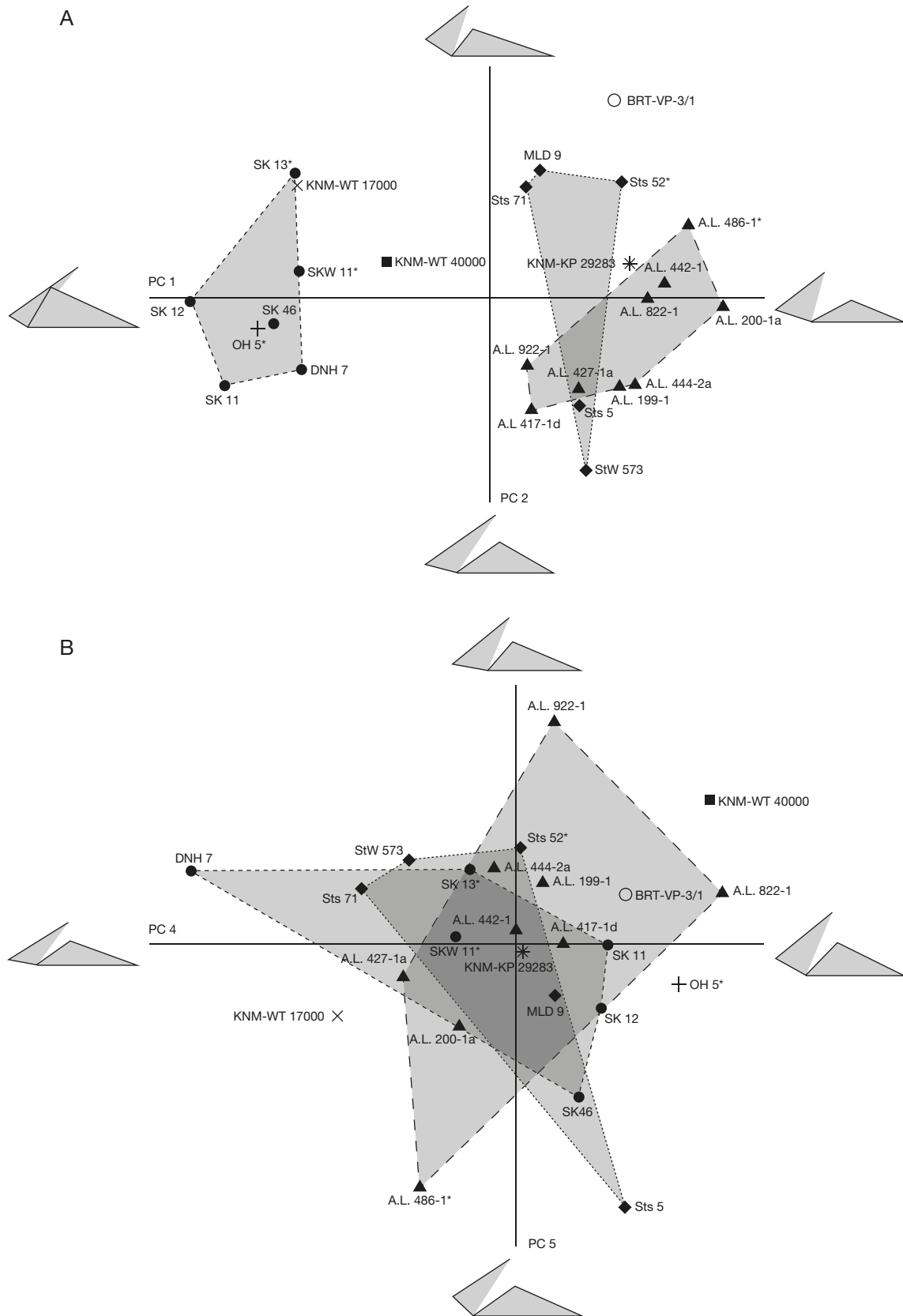
FIG. 3. — Plots of **A**, PC 1 (63%) vs PC 2 (20%) and **B**, PC 4 (5%) vs PC 5 (4%), showing the maxillary shapes of KNM-WT 40000 (**square**), BRT-VP-3/1 (**open circle**), *Australopithecus anamensis* Leakey, Feibel, McDougall & Walker, 1995 (**star**), *A. afarensis* Johanson, White & Coppens, 1978 (**triangles**), *A. africanus* Dart, 1925 (**diamonds**), *Paranthropus aethiopicus* (Arambourg & Coppens, 1968) (**cross**), *P. boisei* (Leakey, 1959) (**plus**), and *P. robustus* Broom, 1938 (**circles**). **Asterisks** indicate late juveniles. Convex hulls are given for *A. afarensis* (**long dashed line**), *A. africanus* (**dotted line**), and *P. robustus* (**short dashed line**). Wireframes are defined in Figure 2D and indicate the extreme shapes of the PC axes.

PC 5 (4% of total shape variance) represents marked variation in prosthion position from more superoposterior for negative scores to more anteroinferior for positive scores (Fig. 3B). Species of *Australopithecus* and *Paranthropus* substantially overlap, with BRT-VP-3/1 falling well within their range. KNM-WT 40000 has the second to highest score, expressing a relatively anteroinferior prosthion position.

Given that PCs 4 and 5 are linked with the position of nasospinale and prosthion, respectively, they jointly express differences in midplane subnasal prognathism in the fossil sample (Fig. 3B). KNM-WT 40000 is characteristically orthognathic, and distinct from other hominins, with two specimens of the highly variable *A. afarensis* sample being closest, followed by BRT-VP-3/1.

PC 6 (2% of total shape variance) represents variation in the relative length of anterior alveolar margin and associated subnasal prognathism. All species overlap and both KNM-WT 40000 and BRT-VP-3/1 fall within their range.

The extent to which the shape differences between KNM-WT 40000 and BRT-VP-3/1 on the one hand, and *A. afarensis*, *A. africanus*, and *P. robustus* on the other are statistically significant was assessed using Mahalanobis distance tests (Table 1). KNM-WT 40000 differs significantly from *A. afarensis* and *A. africanus*, and as indicated by the Procrustes distances, most from the former. However, it does not differ significantly from *P. robustus*, despite being separated from this species on PCs 1, 4, and 5 (Fig. 3). BRT-VP-3/1 differs significantly from *A. afarensis* and *P. robustus*, more from the latter than from the former, but is not significantly different from *A. africanus*, even though it lies outside the range of this species on PC 2 (Fig. 3A).

A specific comparison between the maxillary shape of KNM-WT 40000, BRT-VP-3/1, and the nine *A. afarensis* specimens is shown in Figure 4, with PC 1 (48% of total shape variance) and PC 2 (36% of total shape variance) clearly differentiating between the three. This plot reflects the highly significant differences suggested by the Mahalanobis distance tests (Table 1). The wireframes reinforce that KNM-WT 40000 differs from *A. afarensis* in having a more anterosuperiorly positioned zygomatic process and a longer, more orthognathic subnasal clivus combined with an anteroposteriorly shortening of the anterior maxilla (Fig. 5A). In contrast, BRT-VP-3/1 differs from *A. afarensis* in having a more anteriorly positioned zygomatic process and a shorter subnasal clivus (Fig. 5B).

DISCUSSION

In this study, geometric morphometric analyses are used to examine the maxillary shape of the *K. platyops* holotype KNM-WT 40000 and the *A. deyiremeda* holotype BRT-VP-3/1, expanding on the work of Spoor *et al.* (2010, 2016) by using more accurate data and a larger comparative sample. Comparing these two specimens with the contemporary taxon *A. afarensis*, and with species of *Australopithecus* and *Paranthropus* more broadly, the PCAs in this study yields similar results to those in Spoor *et al.* (2010, 2016), with KNM-WT 40000
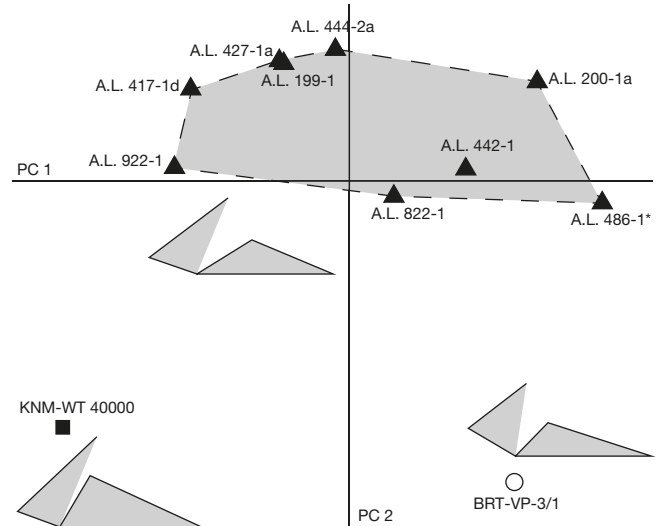

FIG. 4. — Plot of PC 1 (48%) vs PC 2 (36%) showing the maxillary shapes of KNM-WT 40000 (**square**), BRT-VP-3/1 (**open circle**), and *Australopithecus afarensis* Johanson, White & Coppens, 1978 (**triangles**). **Asterisk** indicates the late juvenile and a convex hull is given for *A. afarensis* (**long dashed line**). Wireframes are defined in Figure 2D and show mean shapes for the three groups.

TABLE 1. — Procrustes distances (**PrD**) and squared Mahalanobis distances (**D²**) comparing KNM-WT 40000 and BRT-VP-3/1 with three hominin species, and results of Mahalanobis distance tests, including the standard deviation units (**SDU**), degrees of freedom (**df**), and *p*-values. At *p* < 0.05 two differences are statistically not significant (n.s.).

	PrD	D²	SDU	df	*p*-value
KNM-WT 40000					
Australopithecus afarensis	0.20187	17.157	4.142	6	< 0.005
A. africanus	0.16291	52.017	7.212	5	< 0.0005
Paranthropus robustus	0.12803	12.245	3.499	6	< 0.1 (n.s.)
BRT-VP-3/1					
A. afarensis	0.18484	15.434	3.928	6	< 0.02
A. africanus	0.15692	10.168	3.188	5	< 0.1 (n.s.)
P. robustus	0.31031	55.551	7.453	6	< 0.0005

occupying an intermediate position between *Paranthropus* and *Australopithecus* on PC 1, while BRT-VP-3/1 stands out from the other *Australopithecus* species on PC 2. These PC scores highlight the prominent features that differentiate the KNM-WT 40000 maxilla from *A. afarensis* including a more anterosuperiorly positioned zygomatic process and a longer, more orthognathic, and transversely flat subnasal clivus. For the BRT-VP-3/1 maxilla these are a more anteriorly positioned zygomatic process and a shorter subnasal clivus.

Mahalanobis distance tests show that the differences between KNM-WT 40000 and both *A. afarensis* and *A. africanus* are statistically significant. In contrast, the difference from *P. robustus* is not, even though it is separated from this species on PCs 1, 4, and 5 (Fig. 3). On the other hand, the BRT-VP-3/1 maxilla is significantly different from *A. afarensis* and *P. robustus*, but not from *A. africanus* despite lying outside the range of this

species on PC 2 (Fig. 3A). Comparisons with other species could not be accomplished using Mahalanobis distance tests as each is only represented by a single specimen. Moreover, small sample sizes warrant caution when interpreting the results of the Mahalanobis distance tests. The specimens used in this study may not capture the entire range of variation for a species, although Spoor *et al.* (2010) found that their fossil samples show representative levels of intraspecific morphological variation when compared with much larger samples of modern humans, chimpanzees, and gorillas. Sample size is considered in statistical tests and those employed here are conservative in nature (Spoor *et al.* 2016), thus obtaining statistical significance even with these small samples suggests that the observed differences are considerable. It is furthermore reassuring that the patterns of statical significance align closely with the relationships between fossils in shape space (Fig. 3) and with the Procrustes distances (Table 1).

In addition to assessing how KNM-WT 40000 and BRT-VP-3/1 compare with other hominin species, it is of interest to explore the relationship between the two maxillae, and specifically if their shapes share derived features when compared with *A. afarensis*. Both specimens are significantly different from *A. afarensis*, KNM-WT 40000 more so than BRT-VP-3/1 (Table 1), but importantly, they differ from *A. afarensis* in dissimilar ways. Essentially, BRT-VP-3/1 lacks the more orthognathic and transversely flat subnasal clivus and the superiorly positioned zygomatic process seen in KNM-WT 40000. What appears like a shared feature between these two fossils is the anterior position of their zygomatic process, yet this represents different phenomena, as discussed in Spoor *et al.* (2016). In short, both PC 1 and PC 2 express a shift in the anteroposterior position of the zygomatic process relative to the postcanine tooth row (azp relative to cp3-m2). PC 1 reflects a 'true' change in the position of the zygomatic process, and it is along this axis that KNM-WT 40000 and *Paranthropus* differ from *Australopithecus* (Figs 3A; 5A, C). On the other hand, the shape differences along PC 2 are better characterised as an anteroposterior movement of the full dental arcade relative to the midface as represented by the zygomatic process and the nasal sill (pr-cp3-m2 relative to ns-azp). On this axis, BRT-VP-3/1 is separated from the other *Australopithecus* species, presenting a posteriorly displaced, retracted dental arcade (Fig. 5B, C). Thus, the relevant part of the maxilla that varies along PC 1 is the zygomatic process and along PC 2 it is the dental arcade. This difference is perhaps most effectively demonstrated by the anteroposterior relationship between the zygomatic process and the nasal sill (azp relative to ns), which exhibits strong variation along PC 1 while remaining constant along PC 2 (Fig. 3A). These analyses reconfirm that the KNM-WT 40000 and BRT-VP-3/1 maxillae show a fundamentally different maxillary architecture, despite superficial similarities such as zygomatic root position relative to the postcanine tooth row.

As a broad pattern the diversity in maxillary shape among early hominin taxa is best captured by PCs 1 and 2 (Fig. 3A). However, the similarities in PC 1 scores between KNM-WT 40000 and *Paranthropus* should not be seen in isola-

tion. Rather, they should be considered in combination with PCs 4 and 5, where KNM-WT 40000 is well-separated from *Paranthropus* (Fig. 3B). Jointly these results express that they share a more anterosuperiorly positioned zygomatic process and a longer and transversely flat subnasal clivus, but differ in that KNM-WT 40000 is more orthognathic in the midplane and *Paranthropus* more prognathic. These results are fully consistent with the differential diagnosis of *K. platyops* (Leakey *et al.* 2001).

The most notable differences between the main PCA in this study and those in Spoor *et al.* (2010, 2016) are the consequence of changes in the comparative sample. The *P. robustus* sample is more coherent here, which can mainly be attributed to the changed position of the late juvenile SKW 11 in shape space. Upon investigation, nasospinale was incorrectly marked along the nasal entrance in the digital image used by Spoor *et al.* (2010, 2016), resulting in a shorter subnasal clivus length and hence the more positive PC 2 score for SKW 11 in the previous two studies. This demonstrates the drawback of those studies taking landmarks from 2D digital camera images and using markers to locate nasospinale (Fig. 2B), as opposed to 3D virtual models of reconstructed maxillae. The Drimolen specimen DNH 7, newly included here in the *P. robustus* sample, aligns well with the maxillary architecture shown by the Swartkrans specimens, despite differences in facial morphology (Martin *et al.* 2021; Rak *et al.* 2021). As a result of its addition to the sample and the corrected SKW 11 data, the difference between KNM-WT 40000 and *P. robustus* is not significant here, in contrast to the previous analyses.

Following the addition of two new specimens, Sts 5 and StW 573, the *A. africanus* sample now has a larger range of shape variation than seen in Spoor *et al.* (2010, 2016). These two specimens appear to form a cluster separate from MLD 9, Sts 52, and Sts 71 (Fig. 3A), and possible underlying reasons should briefly be considered. Sts 5 shows remodelling of the anterior alveolar process, associated with developmentally old age (Villmoore *et al.* 2013), but it appears less likely that the height of the postcanine alveolar process would have been affected (Grine *et al.* 2012). Regardless, a more inferior position of the cp3 and m2 landmarks to compensate for alveolar bone loss would only enhance rather than reduce the morphology of a more posterosuperiorly positioned nasal sill and zygomatic process by which Sts 5 stands out along PC 2. Moreover, StW 573 is even more extreme in this morphology, and the analysed right side of this specimen is not affected by age or postmortem damage.

Clarke (2013) has previously suggested that two species can be recognised in the South African *Australopithecus* fossil record, with specimens assigned to *Australopithecus prometheus* Dart, 1948 having a flatter face in comparison with *A. africanus*. However, the two clusters observed here do not particularly differ in subnasal prognathism and do not correspond with Clarke's classification as MLD 9, Sts 71, and StW 573 are assigned to *A. prometheus* and Sts 5 and Sts 52 to *A. africanus* (Clarke & Kuman 2019). Alternatively, the apparent division in the *A. africanus* sample could reflect sexual dimorphism,
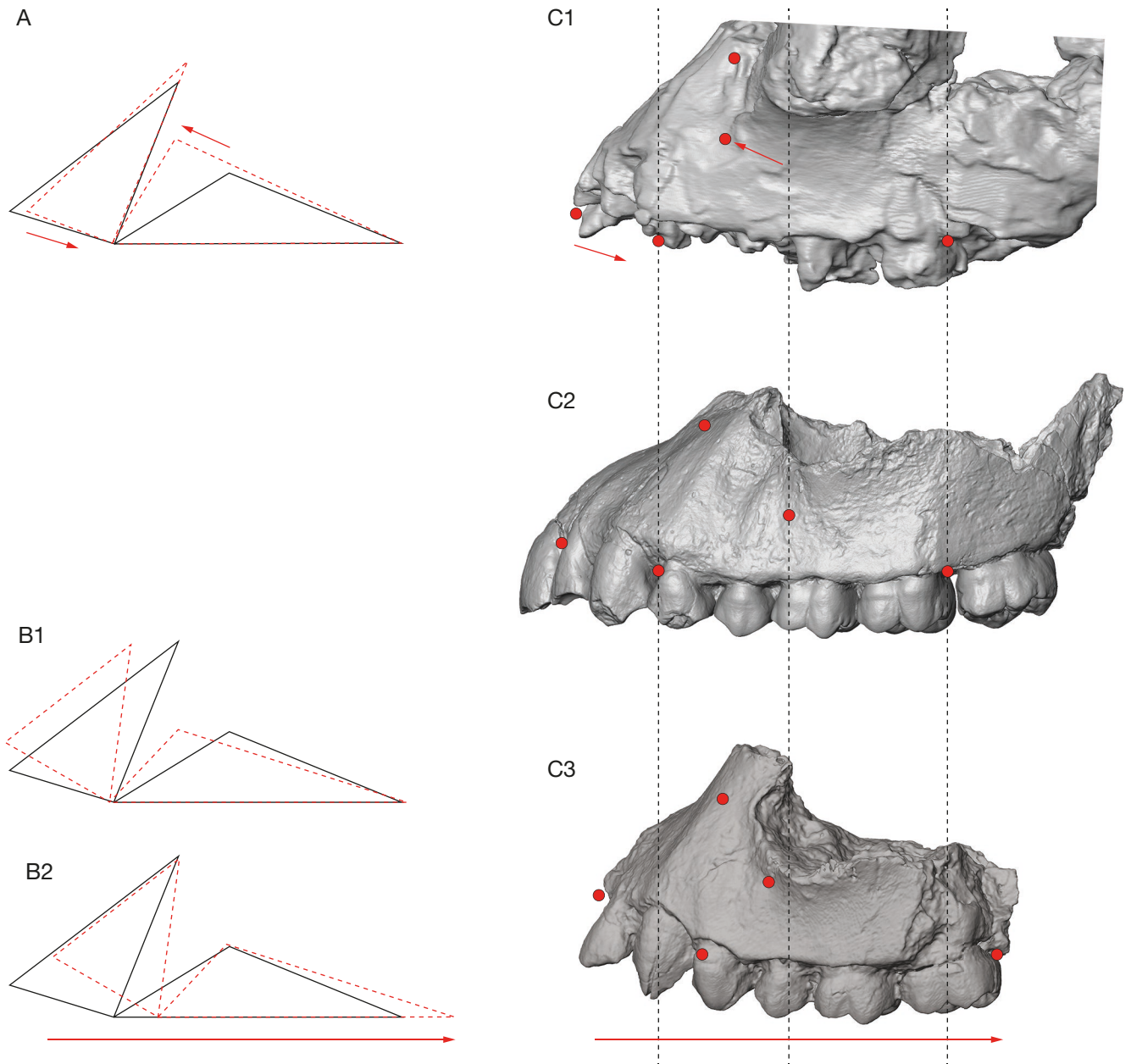
FIG. 5. — **A**, Shape of KNM-WT 40000 (**dashed red line**) compared with the *Australopithecus afarensis* Johanson, White & Coppens, 1978 mean (**black line**) using wireframes as defined in Figure 2D. **Arrows** indicate the shortening of the anterior maxilla and the anterosuperiorly positioned zygomatic process of KNM-WT 4000; **B**, shape of BRT-VP-3/1 (**dashed red line**) compared with the *A. afarensis* mean (**black line**) aligning the wireframes along cp3 and m2 (**B1**) and along ns and azp (**B2**). **Arrow** indicates the posterior shift of the full dental arcade of BRT-VP-3/1; **C**, shape differences between KNM-WT 40000 (**C1**), A.L. 200-1a (**C2**), and BRT-VP-3/1 (**C3**) as described above, shown using 3D surface visualisations scaled to the same cp3 to m2 length. **Red dots** indicate superimposed 2D landmark positions. For KNM-WT 40000 and BRT-VP-3/1 prosthion position is estimated based on morphological clues, and landmark pr therefore does not touch the broken interalveolar septum of these specimens. **Vertical dashed lines** mark the anteroposterior position of landmarks cp3, azp, and m2 for A.L.200-1a.

given that both Sts 5 and StW 573 are considered to be females (Grine *et al.* 2012; Villmoare *et al.* 2013; Crompton *et al.* 2022). However, this factor is difficult to assess, because there is no consensus over the sex of the other *A. africanus* specimens in the sample (Grine *et al.* 2012).

That sexual dimorphism and sex ratio imbalances could bias the findings of this study should also be considered more widely, as they could wrongly be interpreted as taxic diversity. The sex of KNM-WT 40000 is unclear, but Spoor *et al.* (2016) suggested that BRT-VP-3/1 could be a female because of its small size. Our *A. afarensis* sample is represented by at least two males, A.L. 427-1a and A.L. 444-2a, and several females, A.L. 199-1, A.L. 417-1d, A.L. 442-1, and A.L. 822-1 (Johanson *et al.* 1982; Kimbel *et al.* 1994, 2003, 2004; Kimbel & Rak 2010), yet the *A. afarensis* specimens do not plot according to sex in shape space (Fig. 3A). In fact, the two large males A.L. 427-1a and A.L. 444-2a plot closest to A.L. 199-1, the smallest, likely female, specimen in the sample. Apart from SK 13, the Swartkrans *P. robustus* specimens used here were classified as male in Lockwood *et al.* (2007), but the discovery

of the presumptive male cranium DNH 155 at Drimolen has shown that these sex assignments are unreliable (Martin *et al.* 2021). On the other hand, based on its small size it is widely accepted that the DNH 7 skull from Drimolen is female (Lockwood *et al.* 2007; Martin *et al.* 2021; Rak *et al.* 2021). Its maxillary shape plots somewhat marginal to the distribution of the Swartkrans specimens (Fig. 3A), but this could reflect population differences between the two sites (Martin *et al.* 2021) as much as sexual dimorphism. In all, the comparative sample does not provide evidence that sexual dimorphism is a major factor affecting our interpretation of the KNM-WT 40000 and BRT-VP-3/1 specimens.

A second potential source of bias could be that the sample includes some late juveniles. Recently, Hanegraef *et al.* (2022) found that among modern humans and African apes some aspects of the maxilla may show late changes in size and shape, although results are only preliminary due to small samples of late juveniles. In all five extant hominine species the subnasal clivus lengthens from late juveniles to adults and the take-off position of their zygomatic process shows a small but consistent shift in posterior direction along the postcanine dental row (Hanegraef *et al.* 2022), making it plausible that similar changes would have happened among fossil hominin taxa. In contrast, it is less likely that subnasal orientation would have changed notably, given that all extant species other than *Pan paniscus* Schwarz, 1929 show developmental stasis of this particular feature (Hanegraef *et al.* 2022). Age is of particular interest with respect to PC 2 as late juveniles consistently fall at the upper end of their species' distribution on this axis (Fig. 3A). The late juvenile A.L. 486-1 shows the highest PC 2 score of the *A. afarensis* sample, and the same holds true for *P. robustus* with respect to the late juveniles SK 13 and SKW 11. For *A. africanus*, the late juvenile Sts 52 plots at the higher end of this species' variation, but with similar PC 2 scores as the adults Sts 71 and MLD 9. In this context it is important to consider BRT-VP-3/1, as its high PC 2 score could potentially result from its late juvenile status (Haile-Selassie *et al.* 2015). The shape differences expressed on PC 2 match with the ontogenetic changes observed for the extant hominine species, including a shift in subnasal clivus length and anteroposterior position of the zygomatic process, making it plausible that BRT-VP-3/1 would have become more similar to the other *Australopithecus* specimens had it grown up. Moreover, it is worth noting that the current findings reaffirm that the anteroposterior position of the zygomatic process and the subnasal clivus length expressed by PC 1, which differentiates KNM-WT 40000 and *Paranthropus* from *Australopithecus*, are not linked with differences between late juveniles and adults.

In conclusion, the maxillary shapes of KNM-WT 40000 and BRT-VP-3/1 are different from each other and from known *Australopithecus* and *Paranthropus* species, *A. afarensis* in particular, lending further support to the species status of *K. platyops* and *A. deyiremeda* and corroborating the notion that hominin diversity extended well into the mid-Pliocene of eastern Africa (Spoor 2015; Wood & Boyle 2016; Haile-Selassie *et al.* 2016).

REFERENCES

ARAMBOURG C. & COPPENS Y. 1968. — Découverte d'un australopithécien nouveau dans les gisements de l'Omo (Ethiopie). *South African Journal of Science* 64 (2): 58-59. https://journals.co.za/doi/pdf/10.10520/AJA00382353_4440

BROOM R. 1938. — The Pleistocene anthropoid apes of South Africa. *Nature* 142 (3591): 377-379. https://doi.org/10.1038/142377a0

BRUNET M., BEAUVILLAIN A., COPPENS Y., HEINTZ E., MOUTAYE A. H. E. & PILBEAM D. R. 1996. — *Australopithecus bahrelghazali*, une nouvelle espèce d'hominidé ancien de la région de Koro Toro (Tchad). *Comptes Rendus de l'Académie des Sciences, Série IIA, Sciences de la Terre et des Planètes* 322 (10): 907-913. https://gallica.bnf.fr/ark:/12148/bpt6k5752477m

CLARKE R. J. 2013. — *Australopithecus* from Sterkfontein Caves, South Africa, *in* REED K. E., FLEAGLE J. H. & LEAKEY R. E. F. (eds), *The Paleobiology of* Australopithecus. Springer, Dordrecht: 105-123. https://doi.org/10.1007/978-94-007-5919-0_7

CLARKE R. J. & KUMAN K. 2019. — The skull of StW 573, a 3.67 Ma *Australopithecus prometheus* skeleton from Sterkfontein Caves, South Africa. *Journal of Human Evolution* 134: 102634. https://doi.org/10.1016/j.jhevol.2019.06.005

CROMPTON R. H., McCLYMONT J., ELTON S., THORPE S., SELLERS W., HEATON J., PICKERING T. R., PATAKY T., CARLSON K. J., JASHASHVILI T., BEAUDET A., BRUXELLES L., GOH E., KUMAN K. & CLARKE R. 2022. — StW 573 *Australopithecus prometheus*: its significance for an australopith bauplan. *Folia Primatologica* 92 (5-6): 243-275. https://doi.org/10.1159/000519723

DART R. A. 1925. — *Australopithecus africanus*: the man-ape of South Africa. *Nature* 115 (2884): 195-199. https://doi.org/10.1038/115195a0

DART R. A. 1948. — The Makapansgat proto-human *Australopithecus prometheus*. *American Journal of Physical Anthropology* 6 (3): 259-284. https://doi.org/10.1002/ajpa.1330060304

GRANGER D. E., STRATFORD D., BRUXELLES L., GIBBON R. J., CLARKE R. J. & KUMAN K. 2022. — Cosmogenic nuclide dating of *Australopithecus* at Sterkfontein, South Africa. *Proceedings of the National Academy of Sciences of the United States of America* 119 (27): e2123516119. https://doi.org/10.1073/pnas.2123516119

GRINE F. E., WEBER G. W., PLAVCAN J. M. & BENAZZI S. 2012. — Sex at Sterkfontein: 'Mrs. Ples' is still an adult female. *Journal of Human Evolution* 62 (5): 593-604. https://doi.org/10.1016/j.jhevol.2012.01.010

HAILE-SELASSIE Y., SAYLOR B. Z., DEINO A., LEVIN N. E., ALENE M. & LATIMER B. M. 2012. — A new hominin foot from Ethiopia shows multiple Pliocene bipedal adaptations. *Nature* 483 (7391): 565-569. https://doi.org/10.1038/nature10922

HAILE-SELASSIE Y., GIBERT L., MELILLO S. M., RYAN T. M., ALENE M., DEINO A. L., LEVIN N. E., SCOTT G. R. & SAYLOR B. Z. 2015. — New species from Ethiopia further expands Middle Pliocene hominin diversity. *Nature* 521 (7553): 483-488. https://doi.org/10.1038/nature14448

HAILE-SELASSIE Y., MELILLO S. M. & SU D. F. 2016. — The Pliocene hominin diversity conundrum: do more fossils mean less clarity? *Proceedings of the National Academy of Sciences of the United States of America* 113 (23): 6364-6371. https://doi.org/10.1073/pnas.1521266113

HANEGRAEF H. 2023. — *Maxillary morphology of* Australopithecus afarensis *and extant hominines: exploring variation in human evolution*. PhD thesis, University College London, London, 408 p.

HANEGRAEF H., DAVID R. & SPOOR F. 2022. — Morphological variation of the maxilla in modern humans and African apes. *Journal of Human Evolution* 168: 103210. https://doi.org/10.1016/j.jhevol.2022.103210

JOHANSON D. C., WHITE T. D. & COPPENS Y. 1978. — A new species of the genus *Australopithecus* (Primates: Hominidae) from the Pliocene of eastern Africa. *Kirtlandia* 28: 1-14.

JOHANSON D. C., TAIEB M. & COPPENS Y. 1982. — Pliocene hominids from Hadar, Ethiopia (1973–1977): stratigraphic, chronologic, and paleoenvironment contexts, with notes on hominid morphology and systematics. *American Journal of Physical Anthropology* 57 (4): 373-402. https://doi.org/10.1002/ajpa.1330570402

KIMBEL W. H. 2015. — The species and diversity of australopiths, *in* HENKE W. & TATTERSALL I. (eds), *Handbook of Paleoanthropology*. Springer, Heidelberg: 2071-2105. https://doi.org/10.1007/978-3-642-39979-4_50

KIMBEL W. H. & DELEZENE L. K. 2009. — "Lucy" redux: a review of research on *Australopithecus afarensis*. *American Journal of Physical Anthropology* 140 (S49): 2-48. https://doi.org/10.1002/ajpa.21183

KIMBEL W. H. & RAK Y. 2010. — The cranial base of *Australopithecus afarensis*: new insights from the female skull. *Philosophical Transactions of the Royal Society B: Biological Sciences* 365(1556): 3365-3376. https://doi.org/10.1098/rstb.2010.0070

KIMBEL W. H., JOHANSON D. C. & RAK Y. 1994. — The first skull and other new discoveries of *Australopithecus afarensis* at Hadar, Ethiopia. *Nature* 368 (6470): 449-451. https://doi.org/10.1038/368449a0

KIMBEL W. H., RAK Y. & JOHANSON D. C. 2003. — A new hominin skull from Hadar: implications for cranial sexual dimorphism in *Australopithecus afarensis*. *American Journal of Physical Anthropology* 120 (S36): 129. https://doi.org/10.1002/ajpa.10249

KIMBEL W. H., RAK Y. & JOHANSON D. C. 2004. — *The Skull of* Australopithecus afarensis. Oxford University Press, Oxford, 272 p. https://doi.org/10.1093/oso/9780195157062.001.0001

LEAKEY L. S. B. 1959. — A new fossil from Olduvai. *Nature* 184 (4685): 491-494. https://doi.org/10.1038/184491a0

LEAKEY M. G., FEIBEL C. S., MCDOUGALL I. & WALKER A. 1995. — New four-million-year-old hominid species from Kanapoi and Allia Bay, Kenya. *Nature* 376 (6541): 565-571. https://doi.org/10.1038/376565a0

LEAKEY M. G., SPOOR F., BROWN F. H., GATHOGO P. N., KIARIE C., LEAKEY L. N. & MCDOUGALL I. 2001. — New hominin genus from eastern Africa shows diverse middle Pliocene lineages. *Nature* 410 (6827): 433-440. https://doi.org/10.1038/35068500

LEBATARD A.-E., BOURLÈS D. L., DURINGER P., JOLIVET M., BRAUCHER R., CARCAILLET J., SCHUSTER M., ARNAUD N., MONIÉ P., LIHOREAU F., LIKIUS A., MACKAYE H. T., VIGNAUD P. & BRUNET M. 2008. — Cosmogenic nuclide dating of *Sahelanthropus tchadensis* and *Australopithecus bahrelghazali*: Mio-Pliocene hominids from Chad. *Proceedings of the National Academy of Sciences of the United States of America* 105 (9): 3226-3231. https://doi.org/10.1073/pnas.0708015105

LINNAEUS C. 1758. — *Systema Naturae per Regna Tria Naturae: Secundum Classes, Ordines, Genera, Species, cum Characteribus, Differentiis, Synonymis, Locis*. Tomus I. Editio Decima, Reformata. Laurentii Salvii, Holmiae, 824 p.

LOCKWOOD C. A., MENTER C. G., MOGGI-CECCHI J. & KEYSER A. W. 2007. — Extended male growth in a fossil hominin species. *Science* 318 (5855): 1443-1446. https://doi.org/10.1126/science.1149211

MARTIN J. M., LEECE A. B., NEUBAUER S., BAKER S. E., C. S., BOSCHIAN G., SCHWARTZ G. T., SMITH A. L., LEDOGAR J. A. & STRAIT D. S. 2021 — Drimolen cranium DNH 155 documents microevolution in an early hominin species. *Nature Ecology & Evolution* 5 (1): 38-45. https://doi.org/10.1038/s41559-020-01319-6

R CORE TEAM 2023. — R: a language and environment for statistical computing. R Foundation for Statistical Computing, Vienna.

RAK Y., KIMBEL W. H., MOGGI-CECCHI J., LOCKWOOD C. A. & MENTER C. 2021. — The DNH 7 skull of *Australopithecus robustus* from Drimolen (Main Quarry), South Africa. *Journal of Human Evolution* 151: 102913. https://doi.org/10.1016/j.jhevol.2020.102913

SCHWARZ E. 1929. — Das Vorkommen des Schimpansen auf den linken Kongo-Ufer. *Revue de Zoologie et de Botanique Africaines* 16 (4): 425-426.

SPOOR F. 2015. — The middle Pliocene gets crowded. *Nature* 521 (7553): 432-433. https://doi.org/10.1038/521432a

SPOOR F., LEAKEY M. G. & LEAKEY L. N. 2010. — Hominin diversity in the Middle Pliocene of eastern Africa: the maxilla of KNM-WT 40000. *Philosophical Transactions of the Royal Society B: Biological Sciences* 365 (1556): 3377-3388. https://doi.org/10.1098/rstb.2010.0042

SPOOR F., LEAKEY M. G. & O'HIGGINS P. 2016. — Middle Pliocene hominin diversity: *Australopithecus deyiremeda* and *Kenyanthropus platyops*. *Philosophical Transactions of the Royal Society B: Biological Sciences* 371(1698): 20150231. https://doi.org/10.1098/rstb.2015.0231

VILLMOARE B., KUYKENDALL K., RAE T. C. & BRIMACOMBE C. S. 2013. — Continuous dental eruption identifies Sts 5 as the developmentally oldest fossil hominin and informs the taxonomy of *Australopithecus africanus*. *Journal of Human Evolution* 65 (6): 798-805. https://doi.org/10.1016/j.jhevol.2013.09.007

WHITE T. D. 2003. — Early hominids – diversity or distortion? *Science* 299 (5615): 1194-1997. https://doi.org/10.1126/science.1078294

WOOD B. & BOYLE E. K. 2016. — Hominin taxic diversity: fact or fantasy? *American Journal of Physical Anthropology* 159 (S61): 37-78. https://doi.org/10.1002/ajpa.22902

WOOD B. & GRABOWSKI M. 2015. — Macroevolution in and around the hominin clade, *in* SERRELLI E. & GONTIER N. (eds), *Interdisciplinary Evolution Research. Vol. 2. Macroevolution: Explanation, Interpretation and Evidence*. Springer, Berlin: 345-376. https://doi.org/10.1007/978-3-319-15045-1_11

APPENDIX

APPENDIX 1. — Procrustes coordinates. Abbreviations: **azp**, anteroinferior take-off of the zygomatic process; **cp3**, average of the distal canine alveolar margin and mesial third premolar alveolar margin; **m2**, distal second molar alveolar margin; **ns**, nasospinale; **pr**, prosthion.

	ns		pr		cp3		m2		azp	
	X	Y	X	Y	X	Y	X	Y	X	Y
Kenyanthropus platyops Leakey, Spoor, Brown, Gathogo, Kiarie, Leakey & McDougall, 2001										
KNM-WT 40000	0.011	0.374	–0.480	–0.114	–0.211	–0.207	0.702	–0.180	–0.022	0.126
Australopithecus deyiremeda Haile-Selassie, Gilbert, Melillo, Ryan, Alene, Deino, Levin, Scott & Saylor, 2015										
BRT-VP-3/1	–0.118	0.310	–0.504	–0.008	–0.172	–0.187	0.758	–0.161	0.037	0.047
A. anamensis Leakey, Feibel, McDougall & Walker, 1995										
KNM-KP 29283	–0.072	0.279	–0.548	–0.043	–0.203	–0.217	0.703	–0.145	0.120	0.126
A. afarensis Johanson, White & Coppens, 1978										
A.L. 199-1	–0.043	0.327	–0.553	–0.117	–0.223	–0.186	0.663	–0.155	0.157	0.132
A.L. 200-1a	–0.096	0.319	–0.548	–0.072	–0.234	–0.153	0.698	–0.131	0.180	0.037
A.L. 417-1d	0.026	0.371	–0.552	–0.118	–0.233	–0.198	0.654	–0.125	0.105	0.070
A.L. 427-1a	0.008	0.318	–0.567	–0.100	–0.241	–0.187	0.670	–0.114	0.129	0.083
A.L. 442-1	–0.077	0.342	–0.540	–0.079	–0.215	–0.149	0.703	–0.140	0.129	0.026
A.L. 444-2a	–0.025	0.347	–0.575	–0.109	–0.211	–0.163	0.666	–0.130	0.145	0.054
A.L. 486-1	–0.087	0.304	–0.530	–0.020	–0.248	–0.175	0.730	–0.104	0.135	–0.004
A.L. 822-1	–0.082	0.363	–0.537	–0.073	–0.190	–0.197	0.682	–0.160	0.127	0.067
A.L. 922-1	0.009	0.359	–0.561	–0.126	–0.190	–0.171	0.668	–0.150	0.074	0.089
A. africanus Dart, 1925										
MLD 9	–0.066	0.298	–0.495	–0.034	–0.218	–0.209	0.740	–0.152	0.039	0.097
Sts 5	–0.028	0.354	–0.503	–0.108	–0.293	–0.227	0.657	–0.140	0.166	0.121
Sts 52	–0.093	0.323	–0.521	–0.057	–0.191	–0.147	0.738	–0.156	0.066	0.036
Sts 71	–0.052	0.258	–0.509	–0.063	–0.224	–0.173	0.747	–0.155	0.038	0.134
StW 573	0.022	0.302	–0.599	–0.127	–0.224	–0.203	0.637	–0.126	0.164	0.155
Paranthropus aethiopicus (Arambourg & Coppens, 1968)										
KNM-WT 17000	0.050	0.286	–0.451	–0.089	–0.282	–0.195	0.757	–0.143	–0.075	0.141
P. boisei (Leakey, 1959)										
OH 5	0.098	0.380	–0.464	–0.124	–0.263	–0.254	0.683	–0.152	–0.054	0.151
P. robustus Broom, 1938										
DNH 7	0.132	0.324	–0.518	–0.166	–0.284	–0.145	0.700	–0.114	–0.030	0.101
SK 11	0.134	0.404	–0.467	–0.168	–0.282	–0.221	0.671	–0.147	–0.056	0.132
SK 12	0.141	0.350	–0.475	–0.095	–0.259	–0.283	0.694	–0.130	–0.102	0.158
SK 13	0.039	0.321	–0.451	–0.099	–0.245	–0.186	0.753	–0.164	–0.095	0.128
SK 46	0.103	0.384	–0.458	–0.121	–0.293	–0.230	0.694	–0.129	–0.046	0.097
SKW 11	0.071	0.329	–0.470	–0.121	–0.267	–0.202	0.718	–0.149	–0.052	0.143